ARTICLE IN PRESS

Neural Networks ▮ (▮▮▮▮) ▮▮▮–▮▮▮

Contents lists available at SciVerse ScienceDirect

Neural Networks

journal homepage: www.elsevier.com/locate/neunet

2012 Special Issue

# Self-protective whole body motion for humanoid robots based on synergy of global reaction and local reflex

Toshihiko Shimizu [a,b,*], Ryo Saegusa [a], Shuhei Ikemoto [c], Hiroshi Ishiguro [b], Giorgio Metta [a]

[a] Department of Robotics, Brain and Cognitive Sciences, Italian Institute of Technology, Via Morego, 30 16163 Genova, Italy

[b] Department of Systems Innovation, Graduate School of Engineering Science, Osaka University, 1-3 Machikaneyama Toyonaka Osaka 560-8531, Japan

[c] Department of Multimedia Engineering, Graduate School of Information Science and Technology, Osaka University, E6-411 2-1 Yamada-oka Suita Osaka, Japan

ARTICLE INFO

*Keywords:*
Incremental learning
Physical interaction
Force detection
Reflex
Humanoid robot

ABSTRACT

This paper describes a self-protective whole body motor controller to enable life-long learning of humanoid robots. In order to reduce the damages on robots caused by physical interaction such as obstacle collision, we introduce self-protective behaviors based on the adaptive coordination of full-body global reactions and local limb reflexes. Global reactions aim at adaptive whole-body movements to prepare for harmful situations. The system incrementally learns a more effective association of the states and global reactions. Local reflexes based on a force-torque sensing function to reduce the impact load on the limbs independently of high-level motor intention. We examined the proposed method with a robot simulator in various conditions. We then applied the systems on a real humanoid robot.



## 1. Introduction

Self-protection is the most essential motor behavior to assure cognitive humanoid robots' survival in a dynamic environment. In a life-long learning context (Hamker, 2001), the robots should protect themselves from harmful states when physically interacting with the environment. The self-protective response in humans is fast and coordinated even when a collision is not anticipated. As shown in Fig. 1, a person generates a whole body reaction to absorb the impact of a fall. Moreover, human limbs are adjusted to the obstacles by fast motor reflexes and the intrinsic compliance of the musculoskeletal system with contact. In this work, we attempt to create self-protective behaviors for humanoid robots based on this synergistic manner in nature.

In robotics, the subsumption architecture (Brooks, 1991) is traditionally applied to the state-action association of behaviors. In this paradigm, the robot can quickly react to the stimulus, since the sensory input from the environment directly triggers the coupled action from a rich variety of actions. Given this, many studies have focused on reflex-based control. For example, a reflex-based bipedal walking pattern is proposed for the adaptive walk on irregular ground (Huang & Nakamura, 2005) and negotiating a tripping surface (Boone & Hodgins, 1997). Moreover, a reflex-based system was implemented for stabilization of balance (Renner & Behnke, 2006), for bio-mimetic hand control (Folgheraiter, Gini, & Perkowski, 2003), for path planning with collision avoidance (Wikman & Newman, 2002), and for manipulation maintaining human safety (Bauer, Milighetti, Yan, & Mikut, 2010).

Previous studies have mainly focused on generating and maintaining stable controllers, however, they do not consider robots' self-protective movement generation with a high number of degrees of freedom (DOF). We think that self-protection is more important than task operation in facilitating the life-long activity of robots. In this light, reactive behavior should be coordinated adaptively.

We propose a synergistic coordination of precoded local reflexes with incremental learning of global reactions. The learning ability is essential for robots to make use of previous experiences of damage. In contrast, the inherent local reflex supports immature reactions in the early phases of learning. In this article, the reactive behaviors, *reflex* and *reaction*, are quick responses to stimuli: the reflex denotes the precoded behavior and the reaction denotes the adaptive behavior. The proposed system consists of the following features:

- Local reflexes reduce the impact energy of an individual limb.
- Global reactions reduce the total damage of the whole body.
- The reflexes and the initial reactions are precoded.
- The association of novel states with reactions is learned.

We validated the proposed system in experiments with a robot simulation and a physical humanoid robot.

* Corresponding author at: Department of Systems Innovation, Graduate School of Engineering Science, Osaka University, 1-3 Machikaneyama Toyonaka, Osaka 560-8531, Japan. Tel.: +81 06 6850 6360; fax: +81 06 6850 6360.

*E-mail addresses:* shimizu.toshihiko@is.sys.es.osaka-u.ac.jp, toshihiko.shimizu@gmail.com (T. Shimizu), ryos@ieee.org (R. Saegusa).

0893-6080/$ – see front matter © 2012 Elsevier Ltd. All rights reserved.
doi:10.1016/j.neunet.2012.02.011

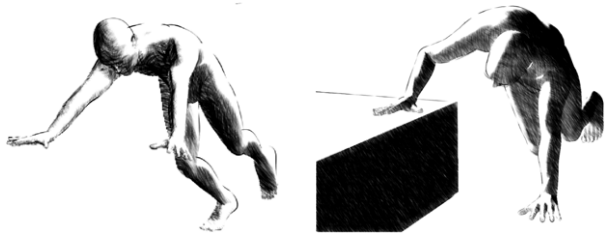

(a) In a flat environment. (b) With obstacles.

**Fig. 1.** Self-protective whole body motions.

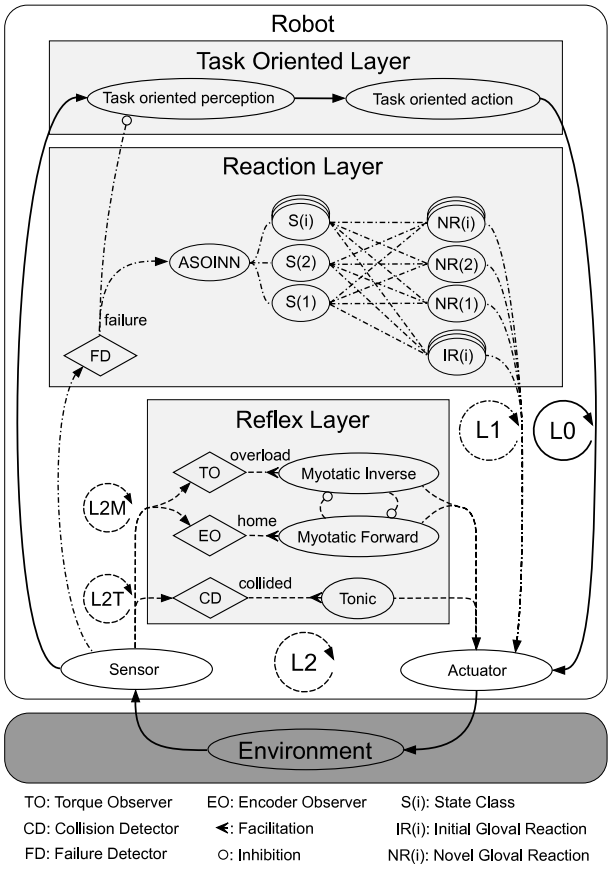


**Fig. 2.** The control diagram of the proposed system. The robot is maintained by the three control layers. The layer L0 is the control loop for a task operation. When the robot detects the danger, the layer L1 is activated to react to it. The neural network ASOINN classifies the states. The layer associates global reactions with the state classes, evaluates the results of these relations over time, and updates the mapping between state classes and reactions whenever the more adequate reaction is found for the class. The reflex layer L2 consists of two control loops L2M and L2T which run independently in individual limbs.

## 2. Reflex based self-protective motion

Fig. 2 shows the control diagram of the proposed system. The system has two self-protective control layers: the reaction layer and the reflex layer, which are superposed on the task-oriented control layer. These control loops continuously observe sensory information to detect potentially harmful states, while the task oriented layer executes a global task such as locomotion or manipulation. The task oriented control loop L0 depicted in Fig. 2 is suppressed by the failure detector (FD) in the reaction layer. The reaction control loop L1 rules the robot until the state is no longer dangerous. The reaction layer generates global reactions by using the whole body in order to reduce prospective damage. The adaptability of global reactions is achieved by robots' incremental learning of the mapping between state classes and reactions with state classification learning and heuristic action learning (details are given in the later sections). The reflex control loop L2 is activated by the collision detector (CD), the torque observer (TO) and the encoder observer (EO) based on force-torque and proprioceptive information. FD and CD are achieved by the change detection of inertial and force-torque information.

### 2.1. Reaction layer

The robot should be able to cope with a variety of harmful states in long-term learning. However, autonomous exploration of the optimum posture for each state from scratch is not practical for high DOF complete humanoid robots. For this reason, we implemented several patterns of self-protective global reactions as initial references in learning. Moreover, the layer associates global reactions with state classes based on the performance of the reactions. The reactions are therefore adaptive and reliable.

The reaction layer classifies a state based on inertial information, body posture, and the relative location of obstacles around the robot. When FD detects a failure, the L0 layer is suppressed, and the sensory state is fed into a state classifier. In order to classify the state, we used a self-organizing incremental neural network (SOINN) (Furao & Hasegawa, 2006), which allows robots to incrementally learn state classification with little memory and few computational requirements. In the proposed system, we used an Adjusted SOINN (ASOINN) (Shen & Hasegawa, 2008) which is an extended version of SOINN with a smaller number of parameters.

#### 2.1.1. Initial global reaction

We implemented four self-protective global reactions as the initial references for the learning (see Fig. 3). The reactions are designed to protect body parts with a priority, the head and the torso first, and the limbs if possible. The reactions have the following features:

- The upper limbs are extended toward the main direction of the fall.
- Lower limbs are folded to reduce the potential energy of the body.
- The neck is stretched towards the opposite direction of the fall.

The first feature is designed to prioritize self-protection. In order to protect the head and torso, the arms or legs should take the role of physical support. The second designed criterion is included to reduce the impact when the robot falls over (Fujiwara et al., 2002). Since the impact depends on the height of the robot's center of gravity, the squatting motion can reduce potential energy. The third feature of this design aims at the safety of the head. The right and left direction of global reactions are basically the same as the front one, but the torso is twisted right and left, respectively.

These precoded reactions are oriented for different falling situations, however, harmful situations occur in myriad ways and are not clearly predictable. Self-protection requires a *universal* reaction. Therefore, we implemented a global reaction with a guard pose to protect the higher priority body parts from all possible impact directions. The guard reaction consists of the following features: the neck is stretched forward; the head is covered by the upper limbs and the lower limbs are folded to reduce the potential energy. The guard reaction is selected when the state is classified as novel.

#### 2.1.2. State definition

The obstacles vary in size, shape, elasticity, etc. The variety of obstacles makes it difficult to describe the relationship between

Please cite this article in press as: Shimizu, T., et al. Self-protective whole body motion for humanoid robots based on synergy of global reaction and local reflex. Neural Networks (2012), doi:10.1016/j.neunet.2012.02.011

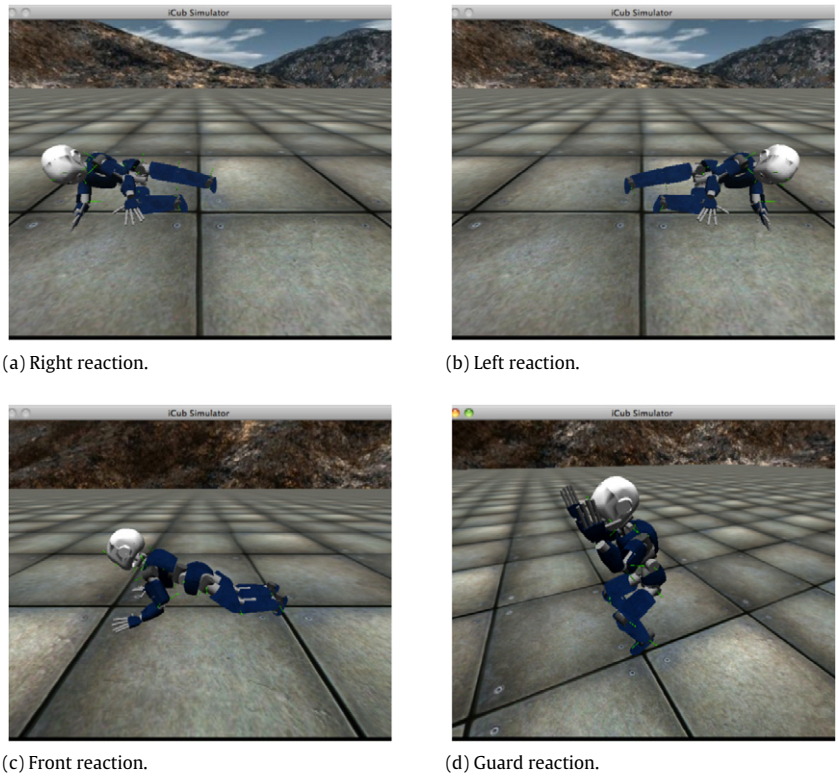


(a) Right reaction. (b) Left reaction.

(c) Front reaction. (d) Guard reaction.

**Fig. 3.** The four self-protective global reactions.

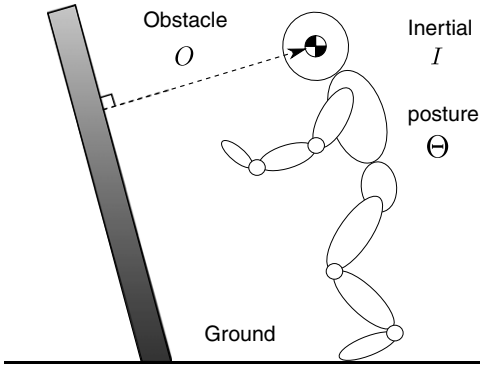


**Fig. 4.** The state definition with an unknown obstacle.

the obstacles and the body. Here, we model a harmful state with the nearest obstacle to the head (see Fig. 4). Note that other body parts such as the hands and legs are excluded from the class of obstacles.

This state definition does not consider prediction (e.g., where the obstacle will be in the near future), or trajectories of obstacles, but considers the instantaneous obstacle characteristics. The self-protective behavior should simply evaluate the state in order to generate a quick response.

The geometry of the obstacle is defined relative to the head's center of mass (COM). The nearest point on the surface of the obstacle is represented as follows:

$$O = \underset{r \in R^O}{\operatorname{argmin}}(|r|), \tag{1}$$

where $R^O$ is a set of the relative positions of obstacle surfaces, and $r = (r_x, r_y, r_z)$ is the relative position of a point in the set.

The whole body posture is defined as follows:

$$\Theta = (\Theta^h, \ldots, \Theta^{rl}), \tag{2}$$

where $\Theta^p = (\theta^p_1, \ldots, \theta^p_{N^p})$ is the posture of body part $p$. $\theta^p_i$ and $N^p$ denote the $i$th joint angle and the total number of joints of $p$, respectively. We assume a set of the body parts $P = \{h, t, la, ra, ll, rl\}$ whose components denote the head, torso, left arm, right arm, left leg and right leg, respectively.

Inertial information is defined as follows:

$$I = (\theta_e, \omega, \ddot{p}) \tag{3}$$

where $\theta_e$, $\omega$, $\ddot{p}$ denotes the Euler angle, angular velocity, and linear acceleration of the robot head, respectively. Finally, the state is represented as follows:

$$X = (O, I, \Theta). \tag{4}$$

In order to measure the state $X$, visual, inertial and proprioceptive sensing are required.

### 2.1.3. Learning of global reaction

The reaction layer organizes the coordination between the global reactions and the state classes given by ASOINN. Here, it is prudent to briefly describe Adjusted SOINN (ASOINN) (Shen & Hasegawa, 2008). ASOINN is a neural network that consists of nodes and links. The nodes and links are reconfigured incrementally to classify input vectors based on geometrical similarity. The nodes in the region with low density are deleted to limit the total number of nodes. ASOINN has two parameters $\lambda$ and $\text{age}_{\max}$, which adjust the frequency of node deletion/removal and old links.

When the state is recognized as a new class, the learning algorithm of the global reaction assigns the guard reaction. When the state is recognized as a known class (not a new class), the algorithm selects a reaction from the initial set. When the algorithm has experienced all initial reactions, protection performance is evaluated and the winning reaction is associated with the state class. After this exploration, the algorithm tries a new reaction for the state class with the exploration rate $\alpha$; i.e., the winning reaction is selected in the probability $1 - \alpha$. The new

Please cite this article in press as: Shimizu, T., et al. Self-protective whole body motion for humanoid robots based on synergy of global reaction and local reflex. Neural Networks (2012), doi:10.1016/j.neunet.2012.02.011

reaction is added to the reaction set only when its performance is better than that of the winning reaction. The learning procedure is presented in Algorithm 1.

**Algorithm 1** Learning the global reaction

**Require:** Reaction set $\Theta_i \in \Theta_R$, basic reaction $\Theta_b$.
1: define $\psi = (c, \Theta, r)$ of the state class $c$, the reaction $\Theta$, and the result $r$ obtained by performing $\Theta$ in $c$. Initialize the set of $\psi$ as $\Psi = \emptyset$.
2: Input new class $c$.
3: if $c$ is the novel class, perform $\Theta_b$ and evaluate the result $r_b$. Then add $\psi = (c, \Theta_b, r)$ to $\Psi$, and go to (2).
4: search $\psi_i$ which have the class $c$ in $\Psi$,
5: **if** The reaction set of the $\psi_i$ is equal to $\Theta_R$ **then**
6: perform the best reaction or the new reaction $\Theta_{i+1}$ by exploration rate $\alpha$. If $r_{i+1}$ obtained by $\Theta_{i+1}$ is better than the best result in the $\psi_i$, add it to $\Theta_R$.
7: **else**
8: perform the unselected reaction $\Theta_i \in \Theta_R$, and add $\psi = (c, \Theta_i, r_i)$.
9: **end if**
10: Go to step (2) to continue the on-line learning.

### 2.2. Reflex layer

Three types of reflexes; the tonic reflex, the myotatic forward reflex, and the myotatic inverse reflex, are managed by the reflex layer. The tonic reflex stops the movement of an individual limb when a collision occurs. The myotatic forward reflex maintains a joint angle to support the body, while the myotatic inverse reflex releases the joint to protect it from overload. Together, the myotatic reflexes locally adjust the stiffness of the joint.

#### 2.2.1. The tonic reflex

The main function of the tonic reflex is to interrupt the movement of a limb colliding with an obstacle. This reflex is triggered only when a collision is detected. The high-stiffness trajectory-based motor control can cause damage for limbs that collide with an obstacle. The movement of the limbs should be modified depending on the state of danger.

#### 2.2.2. The myotatic pair reflex

Joint stiffness should be flexibly controlled to achieve two apparently contradictory tasks, namely, keeping the current joint angles and flowing the overload away from the joints. The key idea here is inspired by the myotatic reflex in humans (Folgheraiter et al., 2003). The human myotatic reflex originates from neuro-muscular fiber function. The main control strategy is the antagonistic feedback control that maintains a joint at a desired position within a safe torque range.

Our myotatic pair reflex is defined as follows:

$$\tau_c^F = \mathrm{PID}(\theta, \theta_d) \quad (\theta \in R_\theta), \tag{5}$$

$$\tau_c^I = 0(\tau \notin R_\tau), \tag{6}$$

where $\tau_c^F$ and $\tau_c^I$ denote the torque command given by the myotatic forward and inverse reflex, respectively. $R_\theta$ represents the position range to evaluate the distance from the home position. $R_\tau$ represents the torque range to judge the safety of the joint torque. Each reflex sends the torque command when the condition is satisfied. *PID* is the function of the PID control and $\theta^d$ denote the desired joint position.

When the torque exceeds the range near the home position, the forward and inverse myotatic reflexes compete with each other, and as a result the joint position is adjusted. Note that these reflexes function in a synergistic manner, even though the reflexes are controlled individually: the applied force are shared with the joints in the same limb and distributed cooperatively in the limb scale.

In the previous work (Shimizu, Saegusa, Ikemoto, Ishiguro, & Metta, 2011), we implemented the flexion reflex that stops joint movement and damps the impact energy. This implementation is a special case of the myotatic pair reflex proposed here. In the flexion reflex, the joint is moved only once upon collision and the posture is fixed after the folding. In contrast, the myotatic pair reflex dynamically maintains the joint position under the external force.

### 2.3. Failure and collision detection

In order to detect the presence of danger, we use Robust Singular Spectrum Transformation (RSST) (Mohammad & Nishida, 2009), which detects the dynamic change of the time sequence of signals. RSST measures the difference between the past and the future at every point of the time sequence. Note that the reference of the future samples in the time window causes a slight delay in detection for the real-time calculation. The theoretical delay is represented as $(n_r + n_c)step$, where $n_r$ and $n_c$ denote the parameters of RSST, and *step* denotes the sampling interval.

## 3. Experiments

The proposed method was evaluated in experiments with a robot simulator and a real humanoid robot. The robot platform is the iCub (Metta, Sandini, Vernon, Natale, & Nori, 2008), a child-scale full-bodied humanoid robot (about 104 cm tall) with 53 DOF (Tsagarakis et al., 2007). The robot platform is controlled with a CPU cluster through the use of the middleware YARP (Metta, Fitzpatrick, & Natale, 2006). In the experiment, we used force-torque sensors mounted on the four limbs (Parmiggiani, Randazzo, Natale, Metta, & Sandini, 2009), an inertial sensor mounted on the head, joint encoders and corresponding motors. In order to observe the applied torque for each joint in TO, we used the iDyn library (Ivaldi, Fumagalli, & Randazzo, 2011) which computes the internal–external torques based on the recursive Newton–Euler algorithm. The simulator platform is compatible with a real robot platform (Tikhanoff et al., 2008).

### 3.1. Simulation experiment

First, we verified the effectiveness of the initial global reactions and the local reflexes under several conditions. Second, we conducted the experiments with learning. We prepared the environmental condition in the simulator as shown in Fig. 5. For simplicity sake, we did not set a specific task for the robot; i.e., the layer L0 was idling. The robot just maintained the standing posture. The robot was pushed from the back, given a linear velocity $\vec{v}_0 = (v_x, v_y, v_z)$ to the torso as shown in Fig. 5(a). We prepared several falls: front, left, right with respective $\vec{v}_0$. We performed 10 trials for each type of fall and calculated the average scores. Table 1 shows the parameters of the experiment.

FD elicits the initial global reactions towards the front, left and right, when the related axis of the head angular velocity $\omega(t) = (\omega_x(t), \omega_y(t), \omega_z(t))$ and the change score of $\omega(t)$ exceed the thresholds. CD elicits the tonic reflex, when the sum of the change scores of the 6 axis force-torque sensor exceeds the threshold. The detection was managed independently in each limb. The applied torque limits for the myotatic pair reflex of each limb were determined experimentally.

Please cite this article in press as: Shimizu, T., et al. Self-protective whole body motion for humanoid robots based on synergy of global reaction and local reflex. Neural Networks (2012), doi:10.1016/j.neunet.2012.02.011

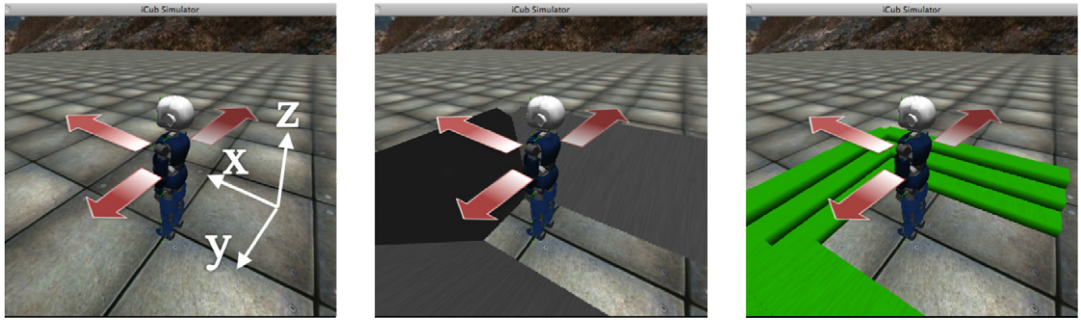


(a) Flat. (b) Slope. (c) Stair.

**Fig. 5.** Environmental conditions for the robot simulator. Figure (a), (b), (c) show the ground conditions of the flat, stair, and slope, respectively.

**Table 1**
Experimental settings for the robot simulation.

| Parameters for directions | | |
|---|---|---|
| Case | FD velocity threshold | Push velocity $\vec{v}_0$ |
| Front | $\omega_y(t) < -10$ deg/s | $(+8, 0, 0)$ m/s |
| Left | $\omega_x(t) < -10$ deg/s | $(0, +8, 0)$ m/s |
| Right | $\omega_x(t) > +10$ deg/s | $(0, -8, 0)$ m/s |
| **Notation of control layer conditions** | | |
| Condition | | Activated control loop |
| No-reaction | | L0 |
| Global | | L0, L1 |
| Global myotatic | | L0, L1, L2M |
| Global tonic | | L0, L1, L2T |
| Global tonic myotatic | | L0, L1, L2M, L2T |
| **Parameters for general setting** | | |
| Parameter of RSST | | $n_r = 5, n_c = 5$ |
| Theoretical delay of RSST | | 0.05 s |
| Change score threshold of CD | | $1e^{-8}$ |
| Change score threshold of FD | | $1e^{-15}$ |
| Time step of simulation | | 0.005 s |
| Time step to elicit reaction | | 0.05 s |
| Time step to elicit reflex | | 0.01 s |

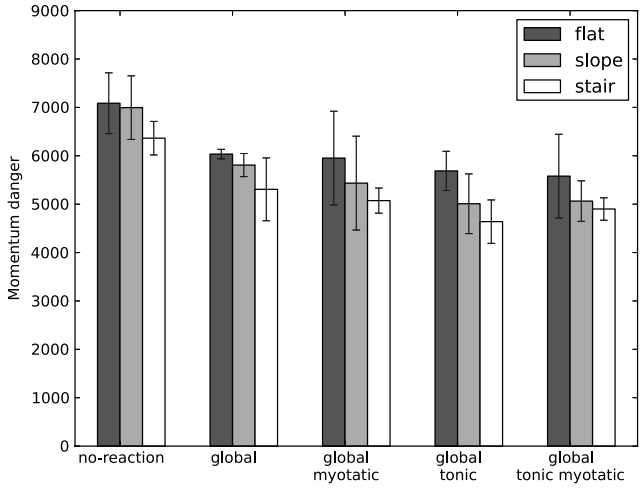


**Fig. 6.** The momentum danger during falling down. The bars show the momentum danger index with the behavior of no reaction, global reaction, global reaction plus tonic reflex, global reaction plus myotatic pair reflex, and global reaction with all reflexes, respectively.

### 3.1.1. Momentum danger index

In order to evaluate the danger for the head during a fall, we referred to the accumulated angular inertia of the head:

$$E^l = \sum_{t=t_s}^{t_e} |\omega(t)|, \tag{7}$$

where $\omega(t)$ denotes the angular velocity of the head at time $t$, $t_s$ and $t_e$ show the start and the end time of the measurement. We set $t_s$ as the start time of the global reaction and $t_e$ as $t_s + 0.5$ s which approximates the time after the collision. We did not consider the mass of the head in Eq. (7) since it was constant during the experiment.

Fig. 6 shows the momentum danger values with respect to the variety of self-protective behaviors. Compared to the condition of no reaction, the proposed system reduced the momentum danger in each self-protective behavior condition. The tonic reflex functioned more effectively than the myotatic pair reflex. The best performance was achieved by the combination of the tonic reflex, the myotatic pair reflex and the global reaction.

### 3.1.2. Energetic safety index

In order to evaluate damage to the most important body parts (i.e., the neck and torso) during a fall, we introduce an energetic safety index as follows:

$$\Gamma = \frac{1}{(w^h \Gamma^h + w^t \Gamma^t)} \sum_{p \in P \setminus \{h,t\}} w^p \Gamma^p, \tag{8}$$

$$\Gamma^p = \frac{1}{t_e - t_s} \sum_{t=t_s}^{t_e} \sum_{i=1}^{N^p} \dot{\theta}_i^p(t) T_i^p(t) dt, \tag{9}$$

where $w^p$ and $\Gamma^p$ denote the priority weight and the normalized driven energy of body part $p$. $\dot{\theta}_i^p(t)$ and $T_i^p(t)$ denote the angular velocity and the applied torque of joint $i$ of body part $p$ at time $t$. In the equations, body part $p = h, t$ denotes the head and torso, respectively. $t_s$ and $t_e$ denote the start and the end time of the measurement. We set them as the start and the end time of the global reaction, respectively.

Fig. 7 shows the energetic safety with respect to the variety of self-protective behaviors. In order to protect the most important body parts, the value of the energetic safety should be higher. The figure shows that the value increased when the global reactions and local reflexes were combined.

The deviation of energetic safety increased when the global reaction was combined with one of the reflexes. In comparison with the index on the direction of a fall, the energetic safety in the front direction was distinctively improved by the combination, which caused the great deviation in energetic safety as we see in the figure.

Note that the myotatic pair reflex distributes concentrated stress over the limb even if the performance is not significant when combined with the tonic reflex. In sum, the result shows that the proposed system protected the most important body parts effectively by distributing the damage over the limbs.

Please cite this article in press as: Shimizu, T., et al. Self-protective whole body motion for humanoid robots based on synergy of global reaction and local reflex. Neural Networks (2012), doi:10.1016/j.neunet.2012.02.011

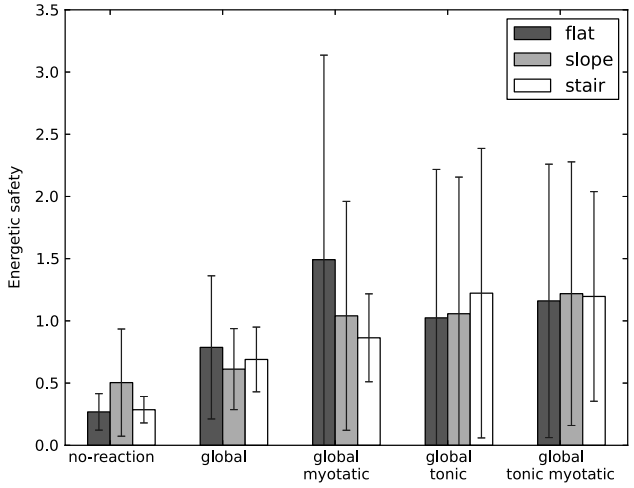


**Fig. 7.** The energetic safety during the falling down. The bars plot the energetic safety index with the behavior of no reaction, global reaction, global reaction plus tonic reflex, global reaction plus myotatic pair reflex, and global reaction with all reflexes, respectively.

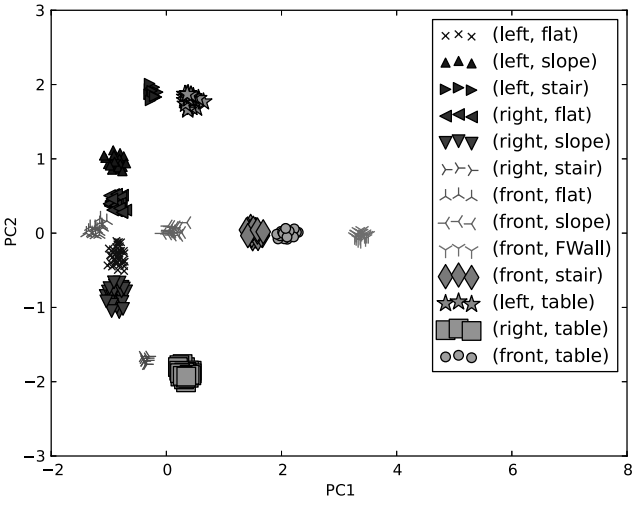


**Fig. 8.** The classification result by ASOINN. PC1 and PC2 denotes the principal components of state $X$. PC1 approximates $r_x$ and $r_z$ of $r$, while PC2 approximates $r_y$ of $r$. $r$ denotes the relative position of the nearest obstacle.

### 3.1.3. Adaptability for novel environments

We investigated the adaptability of self-protective reactions by incremental learning. First, we trained the robot with the ground conditions of flat, slope, and stair as shown in Fig. 5. We pushed the robot in the manner described in Section 3.1. Then, we moved the robot to new environments with front-wall, boxes, and tables as obstacles shown in Fig. 10.

In every condition, we conducted 10 trials. For simplicity, the parameters of ASOINN were set as $\lambda = 100$, $\text{age}_{\max} = 10$, and $\alpha = 0.0$. Other parameters were set as the same values in Table 1. In this experiment, we simplified the state input for ASOINN as $X = O$, since the postural information is theoretically the same in each condition, and the relative locations of the obstacles are more essential than inertial information. The locations of the head and surrounding objects were given by the simulator.

In the initial learning process, the robot was pushed towards the front, left, or right under the conditions of flat, slope, or stair. FD detected failures and the state $X$ was classified by ASOINN. Then, the global reaction coupled with the state class was elicited. In order to train ASOINN with fewer samples, we amplified a single sample as $\lambda$ samples by the normal distribution with the mean as $X$ and the covariance matrix as $0.001I_3$. This is a heuristic to stabilize the classification result with a small number of samples (Sudo, Sato, & Hasegawa, 2009).

Fig. 8 shows the classification result by ASOINN after learning, and Fig. 9 shows the profiles of the momentum danger index during the exploratory learning of the state-action association. In each environmental condition, the system explored all the precoded reactions (i.e., front, left, right, guard reaction) and afterwards assigned the best reactions for the state. In the case of the *box* environment, the system did not need to explore the actions because the state was recognized as a known state class coupled with the front reaction (the state class of the front fall in the slope environment).

### 3.1.4. Action improvements by exploratory learning

We examined learning of the state-action association based on the precoded reactions. We introduced an exploratory learning for the improvement of reactions. In order to enhance the learning speed, we introduced the following heuristics: only pitch joints of the body parts are explored except for the neck, and a symmetric posture is given to the left and right part of the body. The above heuristics limit the exploration to five DOF; the shoulder pitch, elbow pitch, leg pitch, knee pitch, and torso pitch. The other joints were each given a home position. The system generated five random values from the uniform distribution within the feasible joint range, and made up a single full body reaction posture.

We conducted 100 trials of the fall towards the front in the flat ground condition. We then optimized the reaction with the integrated index of the momentum danger as Eq. (7) and the energetic safety as Eq. (8):

$$\text{minimize } w_I \overline{E}^I(\Theta_i) + w_\Gamma / \overline{\Gamma}(\Theta_i), \tag{10}$$

$$\text{subject to } E^I < E_0, \quad \Gamma > \Gamma_0, \tag{11}$$

where $\Theta_i$ denotes the final posture of the reaction. $\overline{E}^I(\Theta_i)$ and $\overline{\Gamma}(\Theta_i)$ represent the normalized value of the momentum danger and the energetic safety of $\Theta_i$. $w_I$ and $w_\Gamma$ denote the weight of $\overline{E}^I(\Theta_i)$ and $\overline{\Gamma}(\Theta_i)$, respectively. We selected the constants as $E_0 = 7000$, $\Gamma_0 = 0.8$ based on the results in Sections 3.1.1 and 3.1.2.

Fig. 11 shows the evaluation of the reactions sampled. The snapshots of the optimum reaction with respect to the momentum danger index ($w_I = 1.0$, $w_\Gamma = 0.0$) and the energetic safety index ($w_I = 0.0$, $w_\Gamma = 1.0$) are shown in Fig. 12(a) and (b). In the optimum momentum reaction, the robot folded its knees and damped the momentum of the body with the arm. In contrast, in the optimum energetic reaction the robot created a posture like a shape of an arc. The manner of this landing dissipated the impact energy. Fig. 12(c) shows the intermediate reaction between the optimum momentum and energetic reaction. As we see in the figure, the reaction balances both the safeguards.

## 3.2. Real-robot experiment

We examined the proposed method with the full-bodied humanoid robot. We mounted the robot on a mobile base in order to create inertial movement and minimize mechanical damage to the robot.

First, we tested failure detection and collision detection by pushing the base from the back. In the test, we set the standing posture as the initial posture of the robot as shown in Fig. 13. The parameters of RSST were set as $n_r = 5, n_c = 5$. The sampling interval of the sensors was about 0.01 s. In this condition, the delay of change score is theoretically 0.1 s. The thresholds of the angular velocity and the change score were set as $\omega_y(t) < -10.0$ deg/s and $1e^{-16}$, respectively.

Please cite this article in press as: Shimizu, T., et al. Self-protective whole body motion for humanoid robots based on synergy of global reaction and local reflex. Neural Networks (2012), doi:10.1016/j.neunet.2012.02.011

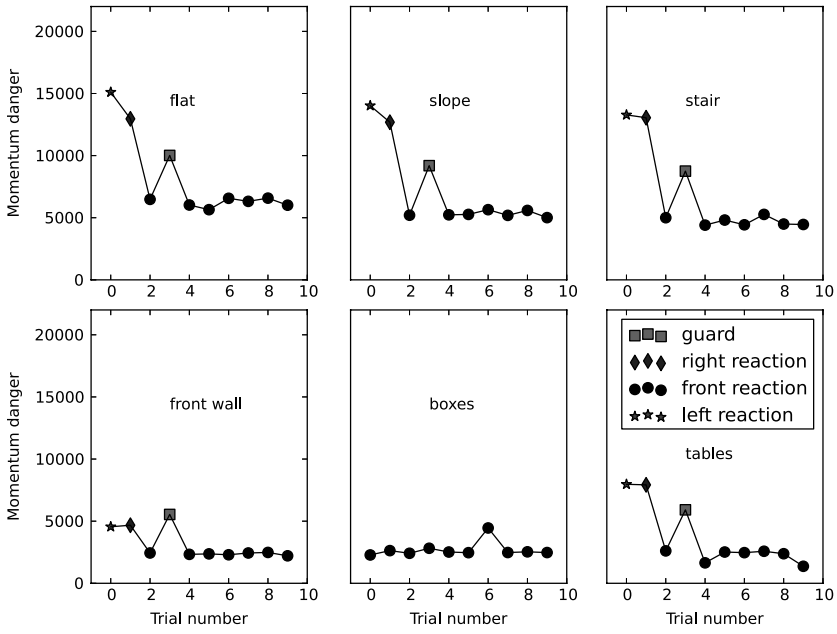


**Fig. 9.** The reaction learning in the case of front falling down.

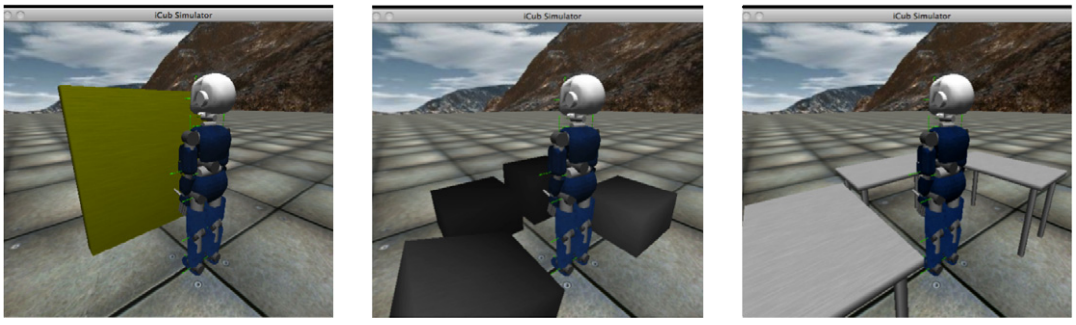

(a) Front wall. (b) Boxes. (c) Tables.

**Fig. 10.** New environments for the simulator. Figure (a), (b), (c) show the ground conditions of the front wall, boxes, and tables, respectively.

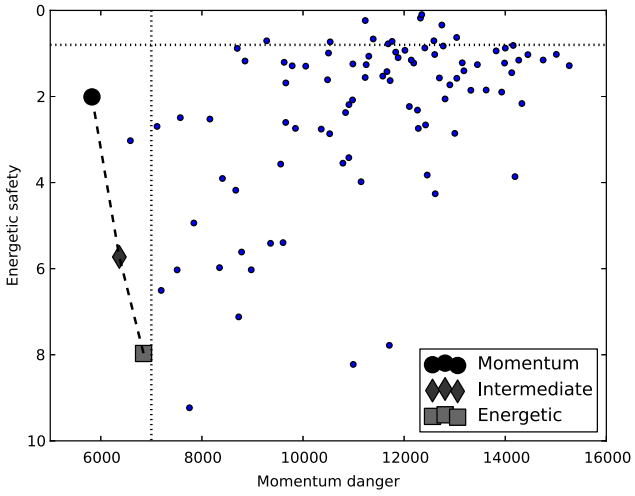


**Fig. 11.** The evaluation of the reactions sampled.

The inertial failure was detected and the frontal global reaction was successfully elicited as shown in Fig. 13. Moreover, during the global reaction the experimenter made contact with the robot. The collision was detected and the tonic reflex was successfully elicited as shown in Fig. 14. Fig. 15 shows the profiles of the force sensors and the change scores when the collision was detected.

We conducted the experiment on the learning of state-action association. In this experiment, an experimenter made contact with the right arm or the right leg of the robot during the motion of the global reaction as shown in Fig. 14. This experimental scenario simulates the collision of the robot with obstacles placed in different locations. The distances from the contact point on the arm and the leg are approximately $|r_a| = 25$ cm and $|r_l| = 50$ cm, respectively.

In order to sample the data for learning and testing, two different experimenters, (A) and (B), demonstrated the actions to make contact with the robot (see Fig. 16 and Fig. 17). For safety reason, all fingers of the robot were folded, and only the guard reaction and the front reaction were set as the alternatives. The exploration of new reactions was excluded in this scenario. We set only the tonic reflex as a local reflex, since the myotatic pair reflex is oriented for collisions with long time intervals (e.g., stabilization after landing), which is not the case of the instantaneous collision that we investigated in this scenario. In each collision condition, the system detected the failure and then one of the reactions was generated. After exploring all the reactions, the system optimized the reaction by the energetic safety index as Eq. (8).

Table 2 shows the result in each condition. In both states of contact (upper arm and upper leg), the front reaction was

Please cite this article in press as: Shimizu, T., et al. Self-protective whole body motion for humanoid robots based on synergy of global reaction and local reflex. Neural Networks (2012), doi:10.1016/j.neunet.2012.02.011

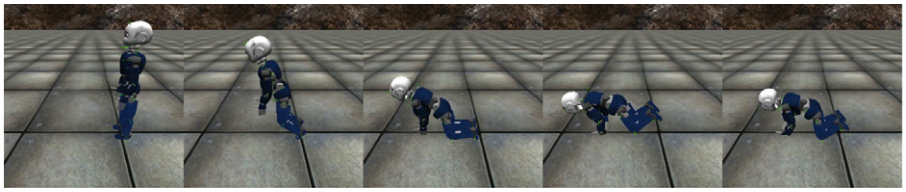

(a) Optimum reaction by the momentum danger index.

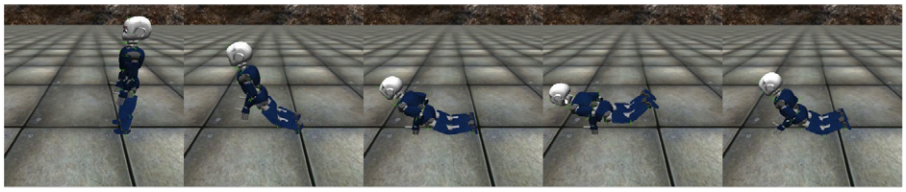

(b) Optimum reaction by the energetic safe index.

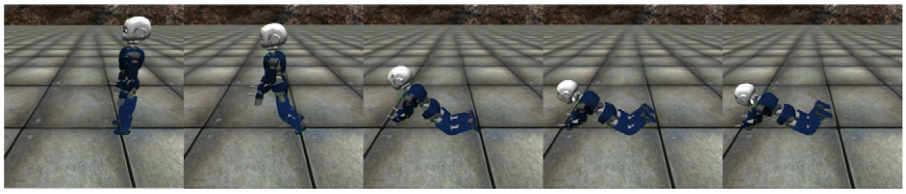

(c) Intermediate reaction by the integrated index.

**Fig. 12.** The snapshots of the optimum reactions.

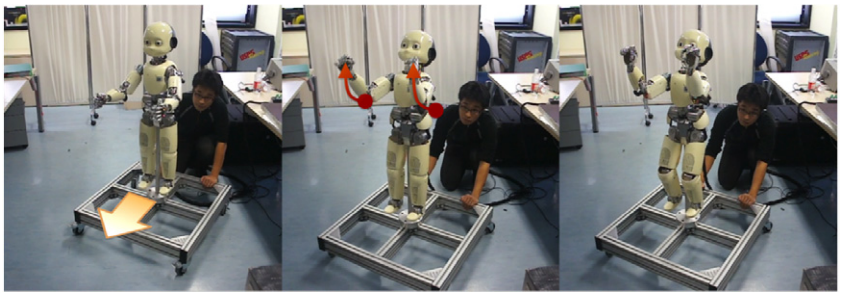

**Fig. 13.** Failure detection and the global reaction elicitation.

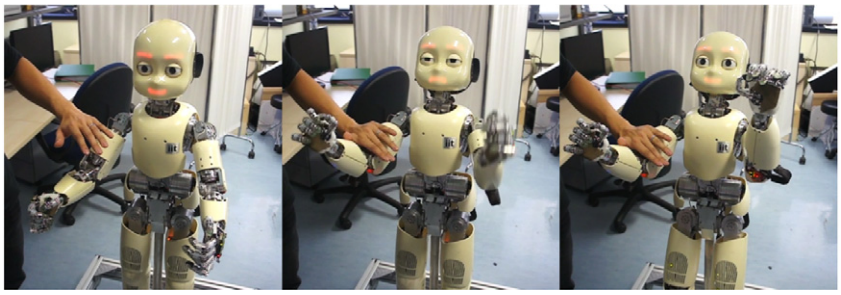

**Fig. 14.** Collision detection and the tonic reflex elicitation.

better than the guard reaction with respect to the energetic safety index. According to the results with experimenter (A), the system assigned the front reaction for the state class as the optimum reaction. Then, experimenter (B) demonstrated the collisions with the robot as shown in Fig. 17, and the system responded to the collision with the same front reaction. As shown in the table, the learned reactions with experimenter (A) marked the best performance in the test with experimenter (B).

Moreover, we tested the independence of the reflex elicitation with successive collisions to different body parts. Fig. 18 shows the snapshots of the multiple collisions. As we see in the figure, the system detected the multiple collisions in different timing, and successfully protected itself by independently eliciting the tonic reflex.

## 4. Discussion

We contrast the proposed system's organization of the pre-coded reflex and adaptive reaction with those of natural systems. Primitive reflexes and postural reactions in humans are generally observed in infancy (Zafeiriou, 2004), and used in pediatrics as the developmental indices of infants. We assume that these reflexes can be inherently implemented in the robot to protect itself from danger. In robotics, the reflex is used as a motor primitive to

Please cite this article in press as: Shimizu, T., et al. Self-protective whole body motion for humanoid robots based on synergy of global reaction and local reflex. Neural Networks (2012), doi:10.1016/j.neunet.2012.02.011

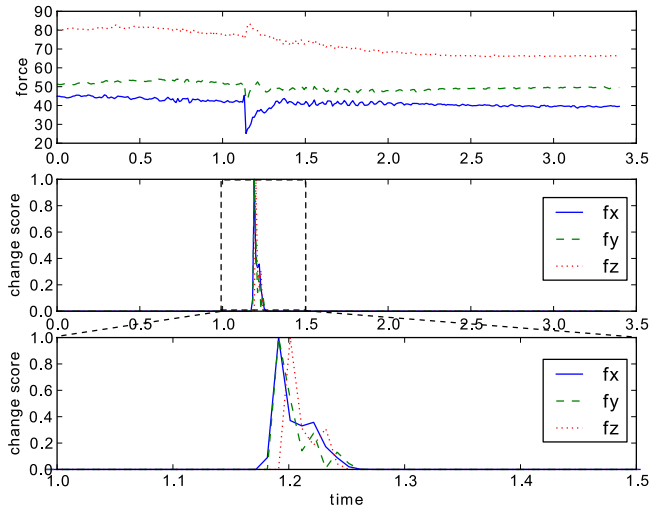


**Fig. 15.** The profiles of force sensors of the right arm. The top figure presents the raw sequence of each sensor axis; the center figure shows the corresponding change scores; the figure in the bottom is the enlargement of the above figure. The change scores are normalized by the local maximum.

**Table 2**
Learning results of the real robot experiment.

| Results with experimenter (A) | | |
|---|---|---|
| Environment | Motion | Energy index |
| Upper arm | Guard | 1.7 |
| Upper arm | Front reaction | 1.9 |
| Upper leg | Guard | 1.4 |
| Upper leg | Front reaction | 2.1 |
| **Results with experimenter (B)** | | |
| Environment | Motion | Energy index |
| Upper arm | Guard | 1.7 |
| Upper arm | Front reaction | 2.0 |
| Upper leg | Guard | 1.4 |
| Upper leg | Front reaction | 2.3 |
| **Summary of the learning and test** | | |
| Environment | Reaction learned in (A) | Reaction elicited in (B) |
| Upper arm | Front reaction | Front reaction |
| Upper leg | Front reaction | Front reaction |

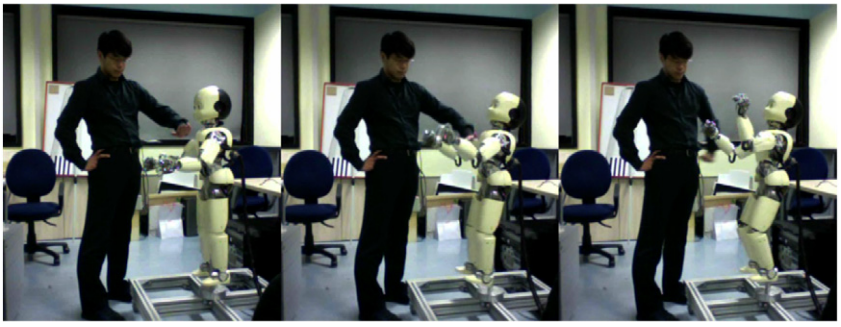

**Fig. 16.** Learning phase of the upper arm collision with experimenter (A). Only the front reaction of the right arm was stopped by the tonic reflex.

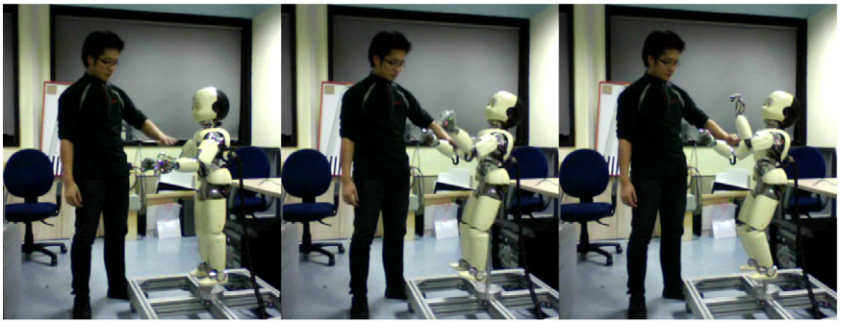

**Fig. 17.** Test phase of the upper arm collision with experimenter (B). The robot recognized the state class and the front reaction was selected. The movement of the right arm was stopped by the tonic reflex as well.

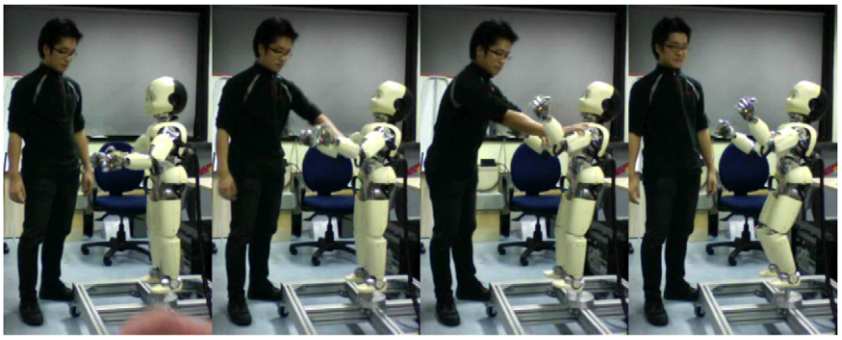

**Fig. 18.** Experiment of multiple collisions. The right and left upper arm were collided with the experimenter (B) successively during the front reaction. The movement of the right and left arm were stopped successively, while both legs kept the moves.

Please cite this article in press as: Shimizu, T., et al. Self-protective whole body motion for humanoid robots based on synergy of global reaction and local reflex. Neural Networks (2012), doi:10.1016/j.neunet.2012.02.011

bind a high number of DOF. Motion generation based on the multiple reflex integration is proposed in Nakamura, Yamazaki, and Mizushima (1999), and extended for task operations in Yoshikai et al. (2003). In contrast to these studies, the proposed method is rather oriented toward self-protection, which overtakes the task operation. We think that the precoded global reactions in the proposed method could be organized more effectively by taking physiological studies into account.

Essentially, the proposed method depends on the ability to detect incoming obstacles. The collision avoidance model in Bermudez i Badia and Verschure (2004) can be applied to make precise detections. We can also enrich the sensory modality of the system with vision and auditory sensing to allow for a multimodal detection of danger. The idea of the auditory-evoked reflex system for a binocular head (Natale, Metta, & Sandini, 2002) is also applicable to the framework of self-protection.

## 5. Conclusions

We proposed a framework of self-protective motor behaviors coordinated with the adaptive global reactions and precoded local reflexes. We experimentally verified the effectiveness of the proposed system with respect to momentum and energetic safety. The results with the robot simulator and the real robot were positive. The system allows the robot to learn the state of danger and new motor skills to protect itself based on an incremental learning scheme. Local reflexes in the limbs support the adaptive reactions to distribute damage.

## Acknowledgments

We would like to appreciate the significant contribution made by Prof. Susan Campbell towards proofreading. This work is partially supported by EU FP7 project CHRIS (Cooperative Human Robot Interaction System FP7 215805).

## References

Bauer, C., Milighetti, G., Yan, W., & Mikut, R. (2010). Human-like reflexes for robotic manipulation using leaky integrate-and-fire neurons. In *Intelligent robots and systems. IROS. 2010 IEEE/RSJ international conference on* (pp. 2572–2577).

Bermudez i Badia, S., & Verschure, P. (2004). A collision avoidance model based on the Lobula giant movement detector (LGMD) neuron of the locust. In *Neural networks., 2004. Proceedings. 2004 IEEE international joint conference on 3, vol. 3* (pp. 1757–1761).

Boone, G., & Hodgins, J. (1997). Slipping and tripping reflexes for bipedal robots. *Autonomous Robots*, *4*(3), 259–271.

Brooks, R. (1991). Intelligence without representation. *Artificial Intelligence*, *47*(1–3), 139–159.

Folgheraiter, M., Gini, G., & Perkowski, M. (2003). Adaptive reflex control for an artificial hand. In *Proc., SYROCO*.

Fujiwara, K., Kanehiro, F., Kajita, S., Kaneko, K., Yokoi, K., & Hirukawa, H. (2002). UKEMI: falling motion control to minimize damage to biped humanoid robot. In *Intelligent robots and systems, 2002. IEEE/RSJ international conference on 3* (pp. 2521–2526).

Furao, S., & Hasegawa, O. (2006). An incremental network for on-line unsupervised classification and topology learning. *Neural Networks*, *19*(1), 90–106.

Hamker, F. (2001). Life-long learning cell structures—continuously learning without catastrophic interference. *Neural Networks*, *14*(4–5), 551–573.

Huang, Q., & Nakamura, Y. (2005). Sensory reflex control for humanoid walking. *IEEE Transactions on Robotics*, *21*(5), 977–984.

Ivaldi, S., Fumagalli, M., & Randazzo, M. (2011). Computing robot internal/external wrenches by means of inertial, tactile and f/t sensors: theory and implementation on the iCub. In *Proc. of the 11th IEEE-RAS international conference on humanoid robots. Bled, Slovenia*.

Metta, G., Fitzpatrick, P., & Natale, L. (2006). YARP: yet another robot platform. *International Journal on Advanced Robotics Systems*, *3*(1), 43–48.

Metta, G., Sandini, G., Vernon, D., Natale, L., & Nori, F. (2008). The iCub humanoid robot: an open platform for research in embodied cognition. In *Proceedings of the 8th workshop on performance metrics for intelligent systems* (pp. 50–56).

Mohammad, Y., & Nishida, T. (2009). Robust singular spectrum transform. *Next-Generation Applied Intelligence*, 123–132.

Nakamura, Y., Yamazaki, T., & Mizushima, N. (1999). Synthesis, learning and abstraction of skills through parameterized smooth map from sensors to behaviours. In *Robotics and automation. 1999. Proceedings. 1999 IEEE international conference on 3, vol. 3* (pp. 2398–2405).

Natale, L., Metta, G., & Sandini, G. (2002). Development of auditory-evoked reflexes: visuo-acoustic cues integration in a binocular head. *Robotics and Autonomous Systems*, *39*(2), 87–106.

Parmiggiani, A., Randazzo, M., Natale, L., Metta, G., & Sandini, G. (2009). Joint torque sensing for the upper-body of the iCub humanoid robot. In *IEEE-RAS international conference on humanoid robots*.

Renner, R., & Behnke, S. (2006). Instability detection and fall avoidance for a humanoid using attitude sensors and reflexes. In *Intelligent robots and systems, 2006 IEEE/RSJ international conference on* (pp. 2967–2973).

Shen, F., & Hasegawa, O. (2008). A fast nearest neighbor classifier based on self-organizing incremental neural network. *Neural Networks*, *21*(10), 1537–1547.

Shimizu, T., Saegusa, R., Ikemoto, S., Ishiguro, H., & Metta, G. (2011). Adaptive self-protective motion based on reflex control. In *International joint conference on neural networks. IJCNN* (pp. 2860–2864).

Sudo, A., Sato, A., & Hasegawa, O. (2009). Associative memory for online learning in noisy environments using self-organizing incremental neural network. *IEEE Transactions on Neural Networks*, *20*(6), 964–972.

Tikhanoff, V., Fitzpatrick, P., Nori, F., Natale, L., Metta, G., & Cangelosi, A. (2008). The iCub humanoid robot simulator. In *International conference on intelligent robots and systems IROS. Nice, France*.

Tsagarakis, N., Metta, G., Sandini, G., Vernon, D., Beira, R., Becchi, F., et al. (2007). iCub: the design and realization of an open humanoid platform for cognitive and neuroscience research. *Advanced Robotics*, *21*(10), 1151–1175.

Wikman, T., & Newman, W. (2002). A fast, on-line collision avoidance method for a kinematically redundant manipulator based on reflex control. *Robotics and Automation*,.

Yoshikai, T., Yoshida, S., Mizuuchi, I., Sato, D., Inaba, M., & Inoue, H. (2003). Multi-sensor guided behaviors in whole body tendon-driven humanoid Kenta. In *Multisensor fusion and integration for intelligent systems. MFI2003. Proceedings of IEEE international conference on* (pp. 9–14).

Zafeiriou, D. (2004). Primitive reflexes and postural reactions in the neurodevelopmental examination. *Pediatric Neurology*, *31*(1), 1–8.

Please cite this article in press as: Shimizu, T., et al. Self-protective whole body motion for humanoid robots based on synergy of global reaction and local reflex. Neural Networks (2012), doi:10.1016/j.neunet.2012.02.011